Axially open nonradiative structures: An example of single-mode resonator based on the sample holder

G. Annino, M. Cassettari, and M. Martinelli

Citation: Review of Scientific Instruments **76**, 084702 (2005); doi: 10.1063/1.1986989
View online: http://dx.doi.org/10.1063/1.1986989
View Table of Contents: http://scitation.aip.org/content/aip/journal/rsi/76/8?ver=pdfcov
Published by the AIP Publishing

Axially open nonradiative structures: An example of single-mode resonator based on the sample holder

G. Annino,[a] M. Cassettari, and M. Martinelli
Istituto per i Processi Chimico-Fisici, Area della Ricerca CNR, via G. Moruzzi 1, 56124 Pisa, Italy

(Received 4 March 2005; accepted 30 May 2005; published online 21 July 2005)

The concept of nonradiative dielectric resonator is generalized in order to include axially open configurations having rotational invariance. The resulting additional nonradiative conditions are established for the different resonance modes on the basis of their azimuthal modal index. An approximate chart of the allowed dielectric and geometrical parameters for the TE_{011} mode is given. A practical realization of the proposed device based on commercial fused quartz capillary tubes is demonstrated at millimeter wavelengths, together with simple excitation and tuning mechanisms. The observed resonances are characterized in their basic parameters, as well as in the field distribution by means of a finite element method. The predictions of the theoretical analysis are well confirmed, both in the general behavior and in the expected quality factors. The resulting device, in which the sample holder acts itself as single-mode resonating element, combines an extreme ease of realization with state-of-the-art performances. The general benefits of the proposed open single-mode resonators are finally discussed. © *2005 American Institute of Physics.*
[DOI: 10.1063/1.1986989]

I. INTRODUCTION

The search for efficient millimeter-wave components such as waveguides, directional couplers, mirrors, gratings, nonreciprocal elements (circulators, Faraday rotators), and resonators have been stimulated by the recent development of versatile solid-state sources. Among the above-mentioned components, the resonators play a fundamental role in all spectroscopic applications, due to the increase of the electromagnetic energy density on the sample and to an effective decoupling of the field distribution from the employed propagation circuit. At millimeter wavelengths the commonly employed resonant devices can be divided in overmoded resonators, like Fabry-Perot cavities[1,2] and whispering gallery mode dielectric resonators,[3] and single-mode ones, such as the well-known TE_{011} cylindrical cavity.[4] The single-mode resonators are considered to have higher power-to-field conversion factors, due to their minimal active volume. In turn they should guarantee the highest absolute sensitivity in any application where the intensity of the electric or magnetic field on the sample is the key parameter. Specific efforts have been devoted to the development of efficient millimeter-wave single-mode resonators.[5–7] The most problematic issues to be faced in this case are given by the size of the resonator, which is of the order of the employed wavelength, and by the feeding and exciting configuration. The commonly proposed solutions, typically borrowed from the microwave technology, are indeed rather difficult to be realized when the wavelength approaches the millimeter. As an example, the typical size of the coupling hole of a TE_{011} cavity working at 100 GHz is of about 0.8 mm. The corresponding thickness of the cavity wall around this hole must be typically less than 0.05 mm.[5] The common requirement of sample manipulation inside the cavity or of its additional irradiation can further complicate the design and the realization of the cavity, leading to performances severely reduced in comparison to the ideal ones. An important application where the above-mentioned aspects are of particular relevance is given by electron paramagnetic resonance (EPR) spectroscopy, which often requires rotation, quick insertion, and substitution of the sample. Here also the use of open cavities is mandatory, since it allows a proper static magnetic field modulation as well as radiofrequency or optical excitation.[6,8,9] A relevant EPR research activity is in particular addressed toward high magnetic fields, where the working wavelengths approach and cross the submillimeter borderline.[1,9–12] For a proper development of millimeter and submillimeter wave single-mode resonators a novel approach seems then mandatory. A recent proposal of single-mode dielectric resonators specifically designed for millimeter-wave applications is reported in Refs. 13 and 14. The room temperature state-of-the-art conversion efficiency has been obtained in a simple structure by using a partially open nonradiative (NR) configuration. The same principle has been extended to metallic resonators, allowing the realization of a widely open TE_{011} cavity.[15] In this reference the possibility of open resonators which combine the benefits of both metallic cavities and dielectric resonators was anticipated. The present article is a further step along this research line, in which the concept of NR resonator is generalized in order to include axially open configurations. In particular, the analysis will focus on single-mode resonances in arbitrarily long dielectric capillary tubes partially shielded by conducting mirrors. In these structures the active region of the resonator can be given by a section of the sample holder itself. The final aim of the article is the demonstration of open single-

[a]Electronic mail: geannino@ipcf.cnr.it

mode resonators having a peculiar ease of realization combined with state-of-the-art performances at millimeter wavelengths. The proposed solutions will be analyzed having in mind possible applications to millimeter-wave EPR spectroscopy. Accordingly, the performances of the resonators will be evaluated in terms of their magnetic field conversion factor.

The scheme of the article is the following. Section II discusses the physical background underlying the realization of a proper axially open NR resonator. The global NR conditions will be established; the related chart of allowed dielectric and geometrical parameters will be given for the TE_{011} mode. In Sec. III a practical realization of the proposed device, based on a commercial fused quartz capillary tube, is investigated at millimeter wavelengths. Possible tuning mechanisms will be demonstrated as well. The expected field distributions, calculated by using a finite element numerical method, are presented in Sec. IV. Finally, Sec. V is dedicated to the analysis of the experimental and computational results, and of their implications.

II. GENERAL ASPECTS

The peculiarity of a NR device is given by its partially open structure, where a region of allowed propagation is surrounded by a (partially open) region of forbidden propagation. A simple application of this principle is given by the NR dielectric resonator,[13] which indeed arose as a logical development of the first proposed NR waveguide.[16,17] Figures 1(a) and 1(b) show a cylindrical version of NR resonator, in which a small central hole is included in order to contain the sample. Here the metallic shielding is given by two plane and parallel mirrors, whose distance is indicated with l. When the diameter of the dielectric disc is of the order of l, the working condition of the resonator can be written as

$$l < \frac{\lambda_0}{2} < l \cdot \sqrt{\varepsilon}, \tag{1}$$

where λ_0 is the wavelength in vacuum corresponding to the resonance frequency and ε the permittivity of the dielectric region. Under the above-noted conditions the central region can contain a resonance mode. The surrounding propagation can only be due to the cutoff-less TEM mode, the parallel-plate TE and TM modes being below their cutoff. Any resonance mode having negligible projection on the TEM mode is thus expected to be unaffected by irradiation losses, provided that the extension of the mirrors is wide enough. This conclusion was experimentally verified on the HE_{111}, TE_{011}, and TM_{011} modes of cylindrical NR dielectric resonators in Refs. 13 and 14. The presence of nonradiating modes can be argued for more general configurations on the basis of rigorous symmetry considerations. Indeed, transverse-electric modes with azimuthal invariance, hereafter referred to as TE_0 modes, are compatible with any configuration having rotational symmetry, as discussed in Ref. 15. The TE_0 modes do not share any field component with the parallel-plate TEM mode (characterized only by axial electric field and azimuthal magnetic field), so at least a nonradiating mode family is expected for any configuration fulfilling the above-

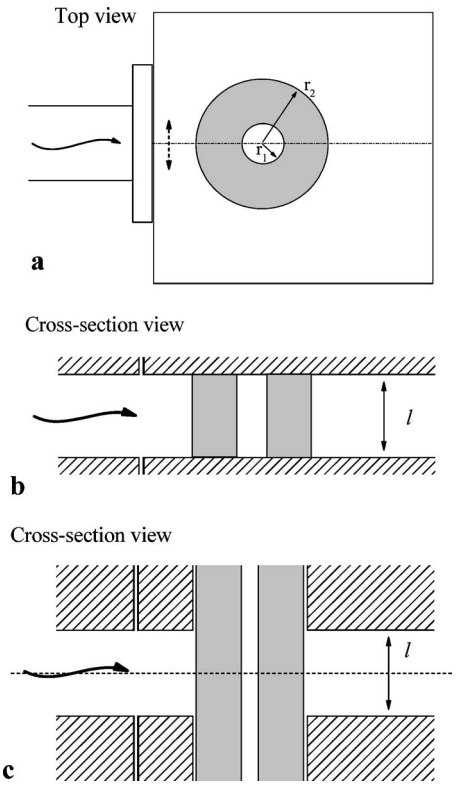

FIG. 1. (a) Top view of a cylindrical NR dielectric resonator with inner radius r_1 and outer radius r_2. The excitation waveguide is shown. (b) Cross-section view of a planar mirrors NR dielectric resonator. The distance between the mirrors is indicated with l. (c) Cross-section view of a possible axially open NR dielectric resonator. The shaded line represents the plane of symmetry of the structure.

mentioned symmetry property. A simple excitation configuration of these resonators can be obtained exploiting their nonradiative character, as discussed in Ref. 13. A radiation incident on the NR structure is indeed totally reflected when its polarization is parallel to the conducting mirrors, provided that the employed wavelength satisfies the NR condition. Only an evanescent field can extend inside the mirrors; this field can transfer energy to the resonator when overlapped with the field of the resonance mode. Once the working frequency and the distance between the mirrors are fixed, the basic parameter that imposes the level of coupling is given by the distance between the incoming radiation and the dielectric region. This parameter can be changed for instance by moving the NR device orthogonally to the incoming radiation, as indicated by the dashed line of Fig. 1(a).[13,14]

The basic NR configuration reported in Figs. 1(a) and 1(b) can be modified as shown in Fig. 1(c), in which the central dielectric disc is replaced by a nominally infinite dielectric tube. The rotational invariance ensures the confinement of the TE_{011} mode along the planar aperture, according to the above-presented NR analysis. A planar confinement is expected for the HE_{111} and TM_{011} modes as well, being the general conditions of symmetry unchanged. The new structure can behave as a proper resonator when the propagation along the dielectric tube is prevented. The analysis of this propagation can be based again on general considerations, in which the symmetry of the structure plays a central role. The resonator can be considered as composed by a central dielec-

tric region in contact with two metallic waveguides partially filled with a dielectric tube. Following the arguments developed for the NR configuration, a resonance mode remains confined in the central region when its projection on the modes propagating along the partially filled metallic waveguides vanishes. The modes propagating along these waveguides can be identified by a pair of indices (n,m), namely an azimuthal index n and a radial index m, due to the axial symmetry of the structure. The symmetry ensures again that only modes having the same azimuthal index can couple to each other.[18] As a consequence, the analysis of the confinement properties will involve only resonant modes of the central region and propagating modes in the adjacent waveguides having the same index n. In the following the different number of modal indices will discriminate between resonant modes and propagating modes.

The fundamental mode of any NR structure is given, as discussed earlier, by the TE_{011} mode. The azimuthally invariant counterpart of the metallic waveguide, assumed here homogeneously filled with a dielectric material, is given by the TE_{0m} family.[4,19] The TE_{011} mode does not share any field component with the other family of modes having vanishing azimuthal index, namely the TM_{0m} family. The cutoff frequencies of the TE_{0m} modes are given by

$$\nu_{\mathrm{TE}_{0m},\mathrm{cutoff}} = \frac{u'_{0,m} \cdot c}{2\pi r_2 \cdot \sqrt{\varepsilon}},$$

where c is the velocity of light in vacuum, ε the permittivity of the dielectric region, r_2 the radius of the waveguide, and $u'_{0,m}$ the nonvanishing roots of the derivative of the first-order Bessel function J_0.[20] The lowest cutoff frequency corresponds to the TE_{01} mode and is given by

$$\nu_{\mathrm{TE}_{01},\mathrm{cutoff}} = \frac{3.8317 \cdot c}{2\pi r_2 \cdot \sqrt{\varepsilon}}.$$

The axial confinement of the TE_{011} mode is then guaranteed provided that $\nu_{\mathrm{TE}_{011}} < \nu_{\mathrm{TE}_{01},\mathrm{cutoff}}$. For a given working frequency the condition of axial confinement can be expressed in terms of the radius of the waveguides as

$$r_{2,\mathrm{TE}_{011}} < \frac{3.8317 \cdot \lambda_0}{2\pi \cdot \sqrt{\varepsilon}}. \tag{2}$$

In order to verify the compatibility of this constraint with Eq. (1), we can go back to the basic structure of Fig. 1(b). The meaning of Eq. (2) can be first investigated on this test configuration. The differences with a true axially open resonator will be discussed later on.

In order to model a realistic NR resonator, the mirrors will be assumed made of aluminum, whose resistivity is equal to 2.8 $\mu\Omega$ cm. The loss factor tan δ of the dielectric region will be assumed equal to 6.7×10^{-4}; its permittivity will be varied from 2 to 11. The resonance frequency of the TE_{011} mode will be fixed to 91.11 GHz. The reason for these somehow arbitrary choices will be cleared up in Sec. III. The dielectric disc will be assumed without central hole for sake of simplicity. By using the above-noted parameters, the resonance frequency, the field distribution, and the merit factor Q_0 of any mode of the resonator of Fig. 1(b) can be calculated following the approach of Ref. 13. In particular, the axial magnetic field conversion factor B_z can be calculated for any allowed pair (l,r_2) imposed by resonance frequency and dielectric permittivity. The curves obtained for the TE_{011} mode are reported in Fig. 2. Here B_z is reported versus the normalized aspect ratio, defined as

$$\frac{l}{\sqrt{\varepsilon} \cdot r_2}.$$

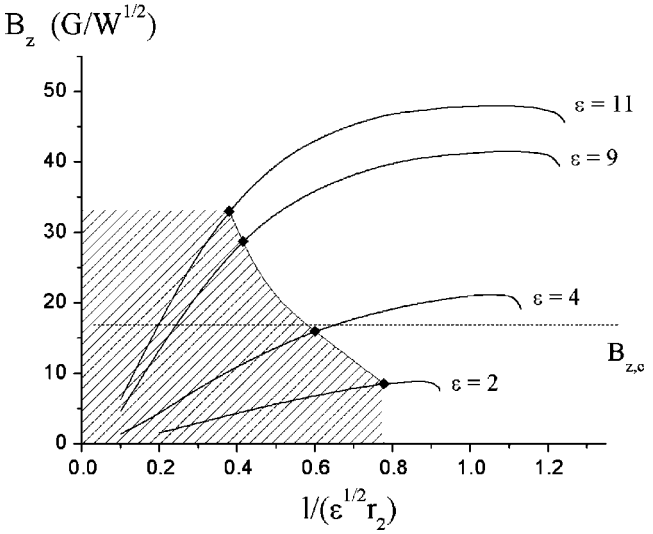

FIG. 2. Chart of the allowed dielectric and geometrical conditions for the TE_{011} mode of an axially open NR resonator. The curves represent the conversion factor B_z vs the normalized aspect ratio, as obtained for the structure of Fig. 1(b). The shaded area indicates the conditions in which the TE_{011} mode of the structure of Fig. 1(c) can leak axially. The dashed line represents the conversion factor B_z of the TE_{011} mode of an ideal aluminum cavity, calculated assuming the optimal aspect ratio $l_c=2r_c$.

For each curve of Fig. 2 the condition

$$r_{2,\mathrm{TE}_{011}} = \frac{3.8317 \cdot \lambda_0}{2\pi \cdot \sqrt{\varepsilon}}$$

is indicated as a diamond. The line which joins the abovementioned points is a guide for the eye, and extrapolates the values given by intermediate permittivity. The shaded region indicates the conditions in which Eq. (2) is not verified or, equivalently, the conditions in which the lowest cutoff frequency of the metallic waveguides is lower than the resonance frequency of the TE_{011} mode. The transformation from the geometry of Fig. 1(b) to that Fig. 1(c) is expected to leave this mode confined in the resonator for any point of the allowed region of Fig. 2, at least under the (unphysical) assumption that this transformation does not modify its resonance frequency. In a realistic case the validity of the abovementioned results can be evaluated by analyzing the resonance frequency variation induced by the axial holes. A possible approach to this problem is based on a perturbative analysis, which gives the frequency variation due to a small deformation of the metallic boundary of the resonator. In particular, the first-order variation of the resonance frequency can be written as

$$\frac{\omega-\omega_0}{\omega_0}=\frac{\int_{\Delta V}(\mu\langle H_0^2\rangle-\varepsilon\langle E_0^2\rangle)dV}{\int_V(\mu\langle H_0^2\rangle+\varepsilon\langle E_0^2\rangle)dV}\ \text{(Ref. 18)},$$

where ΔV is the inward variation of the conducting boundary of the resonator, V is its full volume, and H_0 and E_0 the unperturbed magnetic and electric field. The brackets represent a time average. A reduction of the volume of the resonator leads to an increase of the resonance frequency when the magnetic energy in the removed volume is predominant. In our case this result can be applied to any intermediate configuration between the initial one, represented by Fig. 1(b), and the final one, given by Fig. 1(c). The final result will be obviously independent of the intermediate states, which can be chosen in the most convenient way. We will assume intermediate configurations having cylindrical symmetry, in which the dielectric tube finishes with flat end surfaces; the profile of the mirrors will follow the shape of the tube. The corresponding resonance mode, initially given by the TE_{011} mode, remains of TE_0 nature, thanks to the symmetry of the structure. As a consequence it is characterized by a maximum of magnetic field and a minimum of electric field on the metallic surfaces. For any small elongation of the dielectric tube the resonance frequency decreases, independently of the starting configuration. This allows one to conclude that the above-noted transformation gives a net reduction of the resonance frequency of the TE_{011} mode. This decrease reinforces the axial NR condition, since it reinforces the condition $\nu_{TE_{011}}<\nu_{TE_{01},\text{cutoff}}$. As a consequence, the allowed region shown in Fig. 2 is stable with respect to the transformation of a basic NR structure to the axially open one of Fig. 1(c). It follows that Fig. 2 can be legitimately assumed as an approximate chart of allowed geometrical and dielectric parameters for the TE_{011} mode. This chart suggests a wide range of proper working resonance conditions for axially open resonators. Wider allowed conditions are expected from a more detailed analysis.

The same inductive demonstration could in principle be developed for the other resonance modes. However, the situation is here complicated by the simultaneous presence of electric and magnetic fields on the metallic boundary of the resonator. Being that the other modes are far less important than the TE_{011} one, these modes will be discussed only with generic considerations, postponing further comments after the experimental results. In the case of the TM_{011} mode, the lowest cutoff frequency for the TM_0 counterpart propagating along the circular waveguide is given by

$$\nu_{TM_{01},\text{cutoff}}=\frac{2.4048\cdot c}{2\pi r_2\cdot\sqrt{\varepsilon}},$$

where 2.4048 represents the first root of the Bessel function J_0. The condition $\nu_{TM_{011}}<\nu_{TM_{01},\text{cutoff}}$ is now stronger than that found for the TE_{011} mode. Moreover, simulations and measurements reported in Refs. 13 and 14 show higher resonance frequencies for the TM_{011} mode than for the TE_{011} one. Accordingly, a substantially reduced region of proper resonant conditions is expected here.

In the case of the HE_{111} mode, the lowest cutoff frequency must be chosen among that ones of both the TE_{1m} and TM_{1m} waveguide modes, due to its hybrid nature. The condition to satisfy is now given by

$$\nu_{HE_{111}}<\nu_{TE_{11},\text{cutoff}}=\frac{1.8412\cdot c}{2\pi r_2\cdot\sqrt{\varepsilon}},$$

which corresponds to a quite low cutoff frequency. On the other hand the measured HE_{111} resonance frequencies are much lower than those of the corresponding TE_{011} mode; no clear indications are then possible at this stage.

The above-noted considerations can be generalized to the case of dielectric tubes having finite length. The thickness of the mirrors will still be assumed to be much greater than the extension of the evanescent field. Different cases can be considered. If the axial extension of the tube is much beyond the extension of the evanescent field, its length is obviously irrelevant for the resonance mode. If the tube finishes in the region where the evanescent field is present, a weak effect is expected on the resonance frequencies. On the other hand, the axial confinement of the radiation should be reinforced, due to the increased cutoff frequencies of the empty metallic waveguide. Finally, when the length of the tube is reduced until it finishes inside the mirrors, an abrupt increase of the resonance frequency is expected due to the reduced optical thickness of the resonator.

Having predicted the existence of proper resonant modes in axially open NR structures, the next step concerns a possible excitation scheme. In this respect, the basic similarity between the conventional NR resonators and the axially open one proposed here suggests a direct use of the reflection configuration employed in Ref. 13. A further issue concerns the tuning of the resonance frequency. Two simple approaches can be here envisaged. The first one consists in a reduction of the height of the dielectric tube in the active region of the resonator, as discussed earlier. The second one is based on the variation of the distance between the mirrors.

The following sections will be devoted to the confirmation of the above-mentioned considerations. In the interpretation of the obtained results the help of the basic NR configuration of Fig. 1(b) will be freely invoked.

III. EXPERIMENTAL RESULTS

The material chosen for the dielectric capillary tube was high-purity, ultra-low OH^- content Suprasil® fused quartz, commercially available from Polymicro Technologies, LLC (Arizona, USA). This choice is first motivated by the relatively high permittivity of fused quartz, $\varepsilon\approx 3.8$, which ensures a large region of allowed working conditions as suggested by the chart of Fig. 2. The dielectric absorption is also acceptable; the loss factor is expected indeed lower than 10^{-3} at millimeter wavelengths.[21]

The resonance frequency of the TE_{011} mode will be fixed again at 91 GHz. The approximate size of the dielectric region can be defined with the help of Fig. 2. In particular, inside the allowed area the highest conversion factor is expected for a normalized aspect ratio of the order of unity; the related dimensions are given by $r_2\sim 0.8$ mm and

FIG. 3. (Color online) Picture of the axially open configuration employed in the measurements. The active volume is given by the part of the Suprasil® capillary comprised between the two mirrors.

$l \sim 1.5$ mm. The external diameter of the dielectric tube was then fixed to 1.60 ± 0.01 mm. An internal diameter of 0.40 ± 0.01 mm was chosen in order to obtain a realistic working configuration.

The planar mirrors were realized by means of two rectangular aluminum plates, each 6 mm thick. A series of 1.7 mm holes were drilled in both plates at corresponding positions. Subsequent holes were positioned at increasing distances from the boundary of the plates in order to allow different coupling effectiveness. The chosen diameter allows a comfortable insertion of the dielectric tube. The relatively wide tolerance with respect to the diameter of the tube appears appropriate in view of low temperature applications, since it takes into account the different thermal expansion of fused quartz and aluminum. Moreover, the capability of the resonator to allow a significant degree of mechanical tolerance is a fundamental prerequisite for higher frequency applications. The thickness of the aluminum plates was prudentially assumed quite high, since the evanescent decay of the radiation along the holes can extend in principle over long distances.

In the first measurements the distance l between the mirrors was fixed to 1.65 ± 0.1 mm. A suitable distance between the dielectric tube and the boundary of the mirror was chosen at 1.6 ± 0.1 mm. The final structure of the employed device is reported in Fig. 3. When the above-noted dimensions are assumed for the NR configuration without axial holes, the expected resonance frequencies of the first two modes are given by $\nu_{HE_{111}} = 74.41$ GHz and $\nu_{TE_{011}} = 88.91$ GHz. In these conditions the TM_{011} mode is outside the nonradiative region. Knowledge of these resonance frequencies will give useful information on the effects of the axial holes.

The structure shown in Fig. 3 was investigated in a frequency interval ranging from 50 to 92 GHz. The experimental apparatus and the reflection excitation scheme were the same described in Ref. 13. The coupling of the resonator to the incoming radiation was optimized on the TE_{011} mode. A normalization procedure allowed the extraction of the true

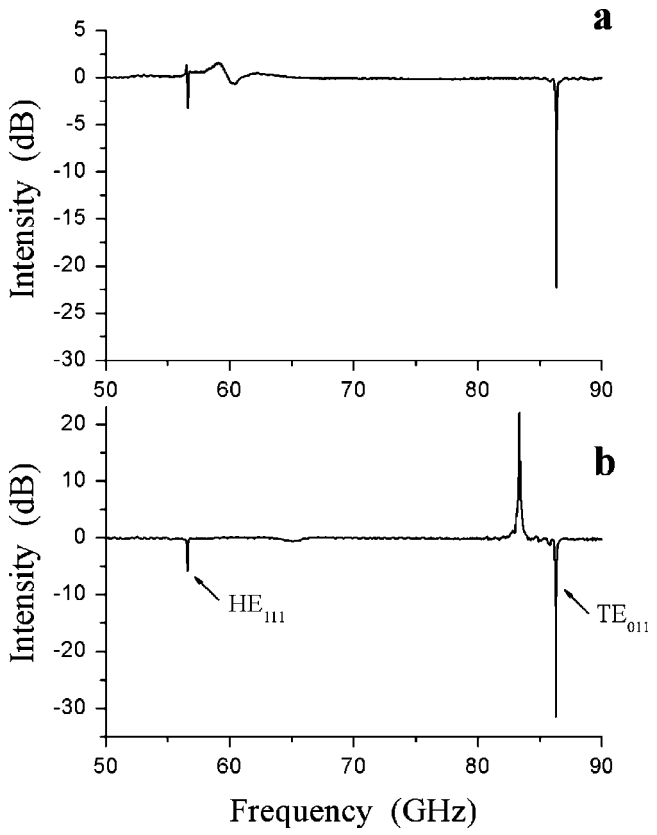

FIG. 4. Normalized spectrum of the resonator of Fig. 3. (a) Normalization obtained displacing the resonating device with respect to the feeding waveguide. (b) Normalization obtained removing the dielectric tube. The assignment of each resonance signal is indicated.

spectrum from the signal background. The reflected signal was first acquired in the proper coupling conditions; the resonator was then completely decoupled from the incoming radiation. The reference signal obtained in this latter condition is finally employed to extract the true spectrum of the resonator. Two different techniques were employed to completely decouple the resonator. The first one consists in the movement of the NR device orthogonally to the incoming radiation, as suggested in Sec. II. The normalized curve obtained in this way is shown in the upper part of Fig. 4. The second procedure for the acquisition of the signal background is simply to remove the dielectric tube. The result of this latter procedure is shown in the lower part of Fig. 4.

The spectra obtained with the above-mentioned procedures show some discrepancy. A crossed comparison allows however a clear identification of the actual resonances with respect to the artifacts introduced by the normalization procedure.[22] All further normalizations will be done removing the resonator. Two resonance modes can be identified in the curves of Fig. 4. The first one, which is supposed to be the HE_{111} mode [following the nomenclature adopted for the configuration of Fig. 1(b)], is centered at 56.58 GHz with coupling of 6.1 dB. The corresponding unloaded merit factor is given by $Q_{0,HE_{111}} = 880$. The axial holes induce here a strong reduction of the resonance frequency with respect to the corresponding configuration without holes. As a consequence a substantial rearrangement of the field distribution is expected. The second resonance, assigned to the TE_{011} mode,

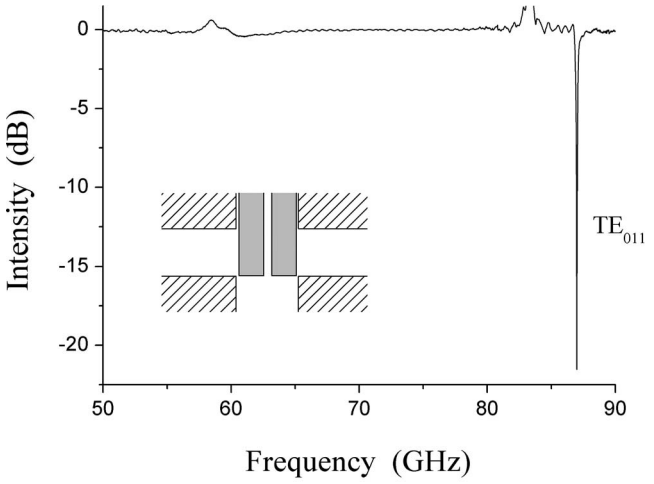

FIG. 5. Normalized spectrum obtained displacing the dielectric tube, as shown in the inset.

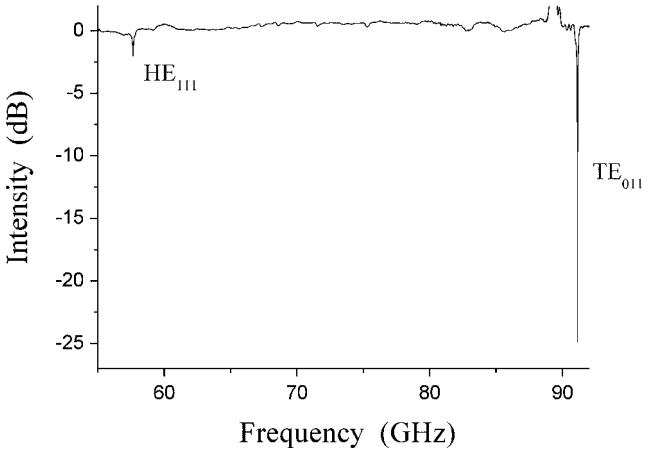

FIG. 6. Normalized spectrum obtained in the configuration of Fig. 3, after a decrease of the distance between the mirrors.

is centered at 86.22 GHz with coupling of 36 dB. The unloaded merit factor is given by $Q_{0,\mathrm{TE}_{011}}=1060$. The moderate resonance frequency reduction here indicates a limited distortion of the electromagnetic field.

In order to verify the tuning procedures proposed in the previous section, the axial position of the quartz tube was displaced until one of its ends was at the same level of the lower mirror, as shown in the drawing of Fig. 5. The resulting spectrum is given by the curve of Fig. 5. The lower frequency resonance disappears, or at least appears as a quite broad line. The TE_{011} mode is, on the other hand, still visible, and centered at 86.92 GHz; the tuning of its resonance frequency was about +0.7 GHz. The coupling of the resonance is 22 dB and the related merit factor $Q_{0,\mathrm{TE}_{011}}=806$. The reduction of this factor can be ascribed to the misalignment of the tube with respect to the axis of the structure. The loss of the axial symmetry generates indeed a mixing among different resonance modes, which in turn open channels for electromagnetic leakage. A similar reason could explain the vanishing of the HE_{111} mode.

In order to test the second tuning mechanism, the distance between the mirrors was reduced to 1.25 ± 0.1 mm. A reduction of the distance between the dielectric tube and the boundary of the mirrors was necessary in order to ensure an efficient excitation of the resonator. A lower distance l leads indeed to higher cutoff frequencies for the parallel-plate TE and TM modes, which increase the decay of the evanescent field outside the dielectric region. A proper distance between the tube and the boundary of the mirror was given by 1.1 ± 0.1 mm. The spectrum of the resonator obtained in this condition is reported in Fig. 6. The HE_{111} and the TE_{011} modes were clearly visible again. The HE_{111} mode was centered at 57.66 GHz; the corresponding unloaded merit factor was $Q_{0,\mathrm{HE}_{111}}=700$. The resonance frequency was then tuned by +1.1 GHz. The TE_{011} mode was centered at 91.11 GHz and tuned by about +5 GHz. Its coupling is about 28 dB; the corresponding unloaded merit factor $Q_{0,\mathrm{TE}_{011}}=1510$.

The previous results give indirect information on the field distribution of both modes. In the case of the HE_{111} resonance, the tuning due to the above-mentioned variation of l is much lower than that induced by the transformation of the structure from a basic NR to an axially open one. This suggests that the rearrangement of the electromagnetic field due to the holes is much higher. The field should then extend much more along the axial holes than outside the dielectric region. In the case of the TE_{011} mode the displacements of the resonance frequency are comparable; the field should then extend comparably in the axial holes and outside the dielectric region.

For ease of comparison, the three TE_{011} modes observed in the investigated configurations are reported in Fig. 7, together with their fit.

In none of the previous measurements was there evidence of the TM_{011} mode, at least in the frequency range of analysis.

IV. NUMERICAL MODELING

Additional information on the observed resonances can be obtained with the aid of computational methods, which can give field distribution, resonance frequency, and quality factor for realistic configurations. The focus will be in par-

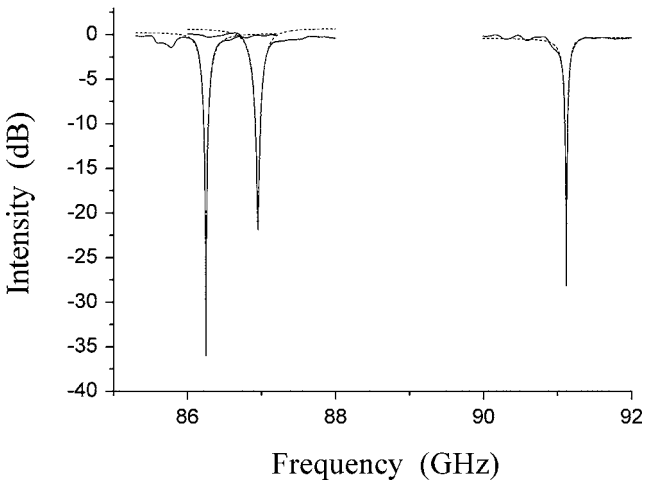

FIG. 7. Detail of the TE_{011} resonances reported in Figs. 4–6, together with their Lorentzian fit.

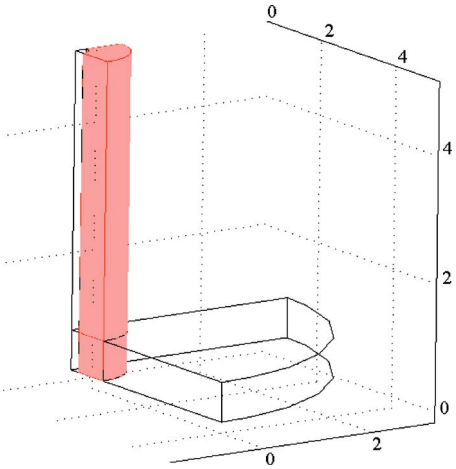

FIG. 8. (Color online) Section of the axially open NR resonator investigated with the finite element method. The shaded area indicates the dielectric region. The unit length is expressed in millimeters.

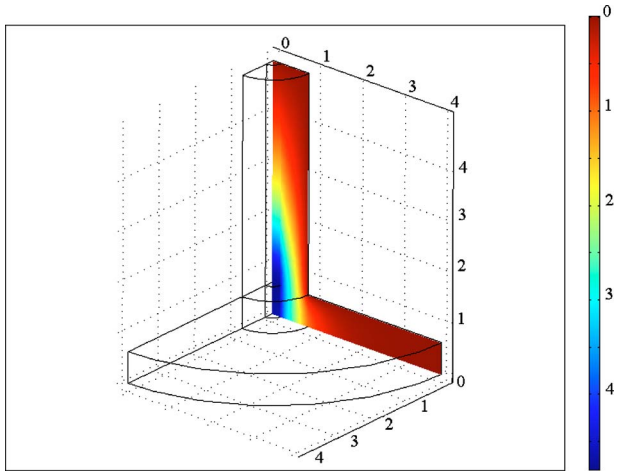

FIG. 9. (Color online) Computed azimuthal electric field of the HE_{111} mode, together with the geometry of analysis. On the right the colors scale, expressed in arbitrary units. The unit length on the axes is expressed in millimeters.

ticular on the resonances of Fig. 6, namely for the case of distance between mirrors equal to 1.25 ± 0.1 mm. The employed software is the finite element method FEMLAB 3.0A (COMSOL, Sweden). A basic parameter of this numerical approach is represented by the number of elementary regions (mesh elements) in the volume of analysis. Better accuracies are in general obtained for an increasing number of mesh elements. Being that this number is limited by practical reasons, it is important to reduce as much as possible the volume of analysis. This can be done by exploiting the symmetry of the problem and the properties of the modes of interest. In our case, these modes are given by the HE_{111}, the TE_{011}, and the TM_{011}. The planar symmetry of the problem can be employed to reduce the modeling to the upper half of the resonator. For the above-presented modes the plane of symmetry can be replaced by a magnetic wall.[18] The rotational invariance can be exploited to limit the analysis to a sector of the full structure. In particular, a quarter of the resonator can be used for all the above-presented modes, provided a proper combination of electric and magnetic walls is used for the radial planes.[23,24] The resulting geometry of analysis is reported in Fig. 8. Here the region of modeling represents an octant of the actual structure. The shaded area indicates the dielectric region.

Some approximations were introduced for sake of simplicity. The external diameter of the dielectric tube was assumed equal to that of the holes, namely 1.7 mm. The internal diameter was assumed equal to 0.4 mm. All corners were considered perfectly sharp. The thickness of the metallic mirrors was finally fixed to 5 mm, instead to 6 mm as in the experimental case. A perfect electric wall was put initially at the end of the axial holes. These assumptions are consistent with the qualitative nature of this computational analysis.

The imposition of boundary conditions suitable for the HE_{111} mode gave a first resonance at 54.54 GHz, whose field distribution is reported in Fig. 9. This solution is then compatible with the low frequency resonance experimentally observed, and already indicated as HE_{111} mode. The electromagnetic field penetrates in a substantial way inside the axial holes, in agreement with the analysis of the previous section. The discrepancy with the measured frequency is most probably due to the simplification operated in the modeling. On the other hand, the obtained field distribution is not influenced by the assumption of holes having finite height. The increase of this height from 5 to 6 mm leaves the calculated resonance frequency stable within 10^{-3}.

The use of boundary conditions compatible with the TE_{011} mode gives a resonance at 91.78 GHz, whose field distribution is reported in Fig. 10. The substantial agreement with the experimental result confirms the assignment of this resonance. In this case the field distribution is essentially limited to the dielectric volume between the conducting mirrors, as suggested in the previous section. The active region of the resonator is then quite small, and similar to that of the corresponding NR configuration without axial holes. The length of the dielectric region and the thickness of the mirrors are now much less critical parameters. It is worthwhile to note that in general the effect of the sample on the field

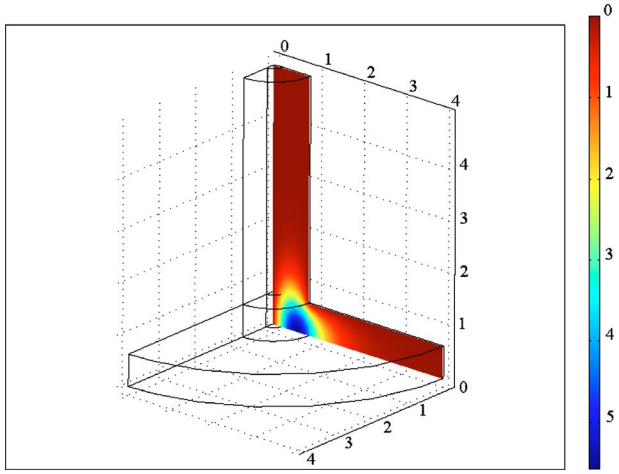

FIG. 10. (Color online) Computed azimuthal electric field of the TE_{011} mode, together with the geometry of analysis. On the right the colors scale, expressed in arbitrary units. The unit length on the axes is expressed in millimeters.

configuration of the TE_{011} mode is negligible, since the sample is placed around a node of the electric field.

A similar analysis was developed for the TM_{011} resonance by imposing the proper boundary conditions. The modeling showed in this case that, when the profile of the resonator is modified from the basic configuration to the axially open one, the mode follows the boundary inside the holes. As a consequence, for the geometry under analysis the TM_{011} resonance cannot be confined in a bounded region.

The above-noted results can be generalized by using a perfect matched layer (PML), which is a nonphysical medium able to absorb almost perfectly the incident radiation.[25] A PML can be used to simulate the behavior of an open structure in finite modeling volumes. In our case possible leakages of radiation can be monitored including proper PML regions far from the expected active volume of the resonator. The results of this analysis confirm that the HE_{111} and the TE_{011} modes do not irradiate appreciably, while the TM_{011} is distorted and absorbed by the PMLs.

V. DISCUSSION

The obtained results confirm the basic predictions formulated in Sec. II. The first two resonance modes of an axially open resonator were observed, namely the hybrid HE_{111} mode and the transverse-electric TE_{011} mode. For the former resonance the experimental and computational results indicate a relevant extension of the fields along the axial holes. This behavior is expected to be peculiar to the HE_{111} mode, due to the low cutoff frequency of the corresponding waveguide TE_{11} mode. The HE_{111} mode is then very sensitive to the diameter of the holes and to the thickness of the mirrors. The extension of the mode inside the holes can be limited reducing the length of the dielectric tube, as confirmed by the numerical modeling.

The TE_{011} mode can be well confined in the dielectric region between the metallic mirrors. This reduced extension gives an additional justification to the chart of Fig. 2, obtained under the assumption that the axial holes introduce a weak perturbation. The minimum overall size of the resonator can be reduced in this case up to few wavelengths without appreciable effects on the confinement of the field. The TE_{011} mode is then an ideal candidate for the realization of single-mode resonators having high conversion factor. The performances of the TE_{011} resonance here observed can be evaluated by resorting again to the NR configuration without holes. The distance between the mirrors can be adjusted until the measured resonance frequency is achieved. The value of l corresponding to 91.11 GHz is given by $l=1.576$ mm. The merit factor of this resonance can be first obtained taking into account the aluminum conductivity only. The value obtained in this way is given by $Q_{0,\mathrm{met}}=5439$. The measured $Q_{0,\mathrm{TE}_{011}}=1510$ can then be reproduced introducing in the modeling a proper dielectric absorption. The loss factor of the Suprasil tube follows as by-product of this procedure. It results $\tan\delta=6.7\times10^{-4}$ around 90 GHz, in agreement with the value given at millimeter wavelengths.[21] Having reproduced the experimental merit factor, the conversion factor can be calculated from the field distribution. The value so obtained, given by $B_z=18\ \mathrm{G/W^{1/2}}$, represents a reasonable estimation of the conversion factor of the employed resonator. The above-mentioned procedure is basically equivalent to assume that the active volume of the actual configuration is the same of that of the model configuration. This approximation is supported by the TE_{011} field distribution shown in Fig. 10. The obtained merit factor and conversion factor can be compared with those of an ideal TE_{011} cavity realized with aluminum. In this case it results $Q_{0,c}=7778$ and $B_{z,c}=16.77\ \mathrm{G/W^{1/2}}$. Similar values have been experimentally demonstrated in Ref. 5. Although the quality factor here obtained is substantially lower than that of the ideal metallic cavity, the conversion factor is expected of the same order or better.[26] This is due to the reduced active volume of a dielectric resonator, which in turn leads to enhanced energy densities. The typical volume of a single-mode dielectric resonator, given by

$$\left(\frac{\lambda_0}{2\cdot\sqrt{\varepsilon}}\right)^3,$$

is in particular about $\varepsilon^{3/2}$ times smaller than that of a metallic cavity working at the same frequency. In particular, a fixed amount of sample inserted in these resonators, characterized by lower active volumes, gives a higher filling factor in comparison to the standard cylindrical TE_{011} cavities.[8]

Despite the extreme ease of realization and the relatively wide mechanical tolerances, the resonator above demonstrated shows state-of-the-art performances at millimeter wavelengths. These performances are mainly limited by the absorption of fused quartz. Better results are expected at lower temperature, where this absorption decreases considerably. The use of better conductors such as copper or silver should give an appreciable quality factor improvement as well. The employment of commercially available dielectric capillary tubes is one of the specific benefits of the proposed configuration. Being that these tubes are available on customer specifications down to an external diameter of $150\pm6\ \mu$m (minimum internal diameter $2\pm1\ \mu$m), the realization of higher frequency single-mode resonators with well-defined properties can be easily accomplished. The identification between resonator and sample-holder opens new possibilities. Among them, the simple and inexpensive replacement of the resonator and the rotation of the sample without need of *ad hoc* designs. The possibility of characterizing different samples inserted along the sample holder can be accounted for as well. In the specific case of EPR spectroscopy also the use of Suprasil seems strategic, since this material is proven free from appreciable paramagnetic impurities also in high-sensitivity instrumentations.[7] The proposed resonator shows all the benefits of a typical NR configuration, as the widely open structure and the presence of few non-degenerate resonance modes. This configuration can be easily generalized following the basic conditions governing the behavior of these rotationally invariant devices, namely

$$l < \frac{\lambda_0}{2}, \quad r < \frac{\bar{u}_{n,m} \cdot \lambda_0}{2\pi \cdot \sqrt{\varepsilon}},$$

where n is the azimuthal modal index of the mode under analysis and $\bar{u}_{n,m}$ a proper root of the first-order Bessel function or of its derivative.

ACKNOWLEDGMENT

The help of C. A. Massa in the preparation of the experimental setup is gratefully acknowledged.

[1] M. R. Fuchs, T. F. Prisner, and K. Moebius, Rev. Sci. Instrum. **70**, 3681 (1999).
[2] A. F. Krupnov, V. N. Markov, G. Y. Golubyatnikov, I. I. Leonov, Y. N. Konoplev, and V. N. Parshin, IEEE Trans. Microwave Theory Tech. **MTT-39**, 284 (1999).
[3] M. E. Tobar, G. L. Hamilton, J. G. Hartnett, E. N. Ivanov, D. Cros, and P. Guillon, Meas. Sci. Technol. **15**, 29 (2004).
[4] H. A. Atwater, *Introduction to Microwave Theory* (McGraw-Hill, New York, 1962).
[5] O. Burghaus, M. Rohrer, T. Gotzinger, M. Plato, and K. Moebius, Meas. Sci. Technol. **3**, 765 (1992).
[6] G. Janssen, A. Bouwen, P. Casteels, and E. Goovaerts, Rev. Sci. Instrum. **72**, 4295 (2001).
[7] H. Blok, J. A. J. M. Disselhorst, S. B. Orlinskii, and J. Schmidt, J. Magn. Reson. **166**, 92 (2004).
[8] C. P. Poole, *Electron Spin Resonance: A Comprehensive Treatise on Experimental Techniques* (Wiley, New York, 1983).
[9] H. Blok, J. A. J. M. Disselhorst, H. Van der Meer, S. B. Orlinskii, and J. Schmidt, J. Magn. Reson. **173**, 49 (2005).
[10] J. P. Barnes and J. H. Freed, Rev. Sci. Instrum. **68**, 2838 (1997).
[11] Y. A. Grishin, M. R. Fuchs, A. Schnegg, A. A. Dubinskii, B. S. Dumesh, F. S. Rusin, V. L. Bratman, and K. Moebius, Rev. Sci. Instrum. **75**, 2926 (2004).
[12] T. A. Konovalova, J. Krzystek, P. J. Bratt, J. van Tol, L. C. Brunel, and L. D. Kispert, J. Phys. Chem. B **103**, 5782 (1999).
[13] G. Annino, M. Cassettari, M. Martinelli, and P. J. M. van Bentum, Appl. Magn. Reson. **24**, 157 (2003); *ibid.* **26**, 458 (E) (2004).
[14] G. Annino, M. Cassettari, and M. Martinelli, Appl. Magn. Reson. **26**, 447 (2004).
[15] G. Annino, M. Cassettari, and M. Martinelli, physics/0408130 (2004); G. Annino, M. Cassettari, and M. Martinelli, Rev. Sci. Instrum. **76**, 064702 (2005).
[16] T. Yoneyama and S. Nishida, IEEE Trans. Microwave Theory Tech. **MTT-29**, 1188 (1981).
[17] T. Yoneyama, in *Infrared and Millimeter-Waves*, edited by K. J. Button (Academic, New York, 1984), Vol. 11, pp. 61–98.
[18] D. Kajfez and P. Guillon, *Dielectric Resonators* (Artech House, Dedham, 1986).
[19] This analysis can be developed in the same way for partially filled waveguides by using the right cutoff frequencies and field distributions, as calculated for instance in K. A. Zaki and A. E. Atia, IEEE Trans. Microwave Theory Tech. **MTT-31**, 1039 (1983).
[20] J. A. Stratton, *Electromagnetic Theory* (McGraw-Hill, New York, 1952), Chap. 9.
[21] J. M. Dutta, C. R. Jones, and H. Davé, IEEE Trans. Microwave Theory Tech. **MTT-34**, 932 (1986).
[22] The positive peak in the lower curve of Fig. 4 is most likely due to a resonant leakage through the axial holes, which appears in absence of the dielectric tube.
[23] G. Annino, M. Cassettari, and M. Martinelli, Appl. Magn. Reson. **20**, 97 (2001).
[24] For the rotationally invariant TE_{011} and TM_{011} modes the volume of analysis can be arbitrarily reduced. The proposed solution is however compatible with all modes of interest, as discussed in the text.
[25] J. Jin, *The Finite Element Method in Electromagnetics* (Wiley, New York, 2002).
[26] In specific applications, such as pulsed magnetic resonance, resonators having high conversion efficiencies for low merit factors represent the most appropriate solution, since they combine high sensitivity with low dead time. In this case, the small active region of the TE_{011} mode, lower than that of a standard TM_{011} cavity, allows the insertion of the sample in the volume of maximum homogeneity of the static magnetic field also when the sample fills the whole capillary.